JOURNAL OF MATERIALS SCIENCE 23 (1988) 3792–3799

Shear testing of mercuric iodide single crystals*

GARY GEORGESON, FREDERICK MILSTEIN
Departments of Materials and Mechanical Engineering, University of California, Santa Barbara, CA 93106, USA

A specialized shear testing system has been designed and assembled for the purpose of measuring the response of thin single crystals of mercuric iodide to shear loading. Numerous stress–strain measurements have been made on single crystal samples of thicknesses ranging from 0.3 to 1.0 mm. Shear strains of over 100% are readily achieved. The results are analysed in terms of a two-parameter semiempirical model for yielding that fits the experimental data extremely well. The model employs a normalized Gaussian distribution $f(s)$ for the change $f(s)ds$ in the relative density of mobile dislocations that occurs when the shear stress s is increased from s to $s + ds$. The Gaussian parameters s_0 (the shear stress at which the density of mobile dislocations has reached half its steady state value) and σ (the standard deviation) are determined from a least squares fit of the theoretically computed stress–strain curve to the experimental data. The "onset of yielding" s_c is defined as $s_0 - 2\sigma$, which is the shear stress at which the density of mobile dislocations has reached about 2% of its steady state value. The utility of the model for studying work hardening and time dependent recovery in single crystal HgI_2 is established.

1. Introduction

Plastic deformation in single crystal mercuric iodide (HgI_2) was first studied systematically by James and Milstein [1, 2]. Owing to the relatively small size of available crystals (and to the crystals' softness and chemical reactivity), James and Milstein [2] designed and built a specialized micromechanical compression testing apparatus for use in their experimental programme. Their apparatus was also used by Milstein and coworkers [3] to investigate the influence of temperature upon the elastic limit of single crystal HgI_2 in compression. Georgeson and Milstein [4] designed and built special specimen grips to eliminate end effects associated with non-uniform bending and rotation in tensile and compression testing of small single crystals. These were used by Milstein and Georgeson [5], in conjunction with James and Milstein's apparatus, to determine the response of single crystal HgI_2 to uniaxial tensile and compressive loading. Although these testing systems enabled the general plastic response of single crystal HgI_2 to be determined, a major drawback is that they are not suitable for the testing of thin specimens (say of thickness 1 mm or less). This is important because the practical application of HgI_2 is for the fabrication of radiation detectors, which are in the form of thin slabs (typically 1 mm or less thickness), and for reasons which are indicated here, it is desirable to characterize the mechanical properties of the detectors themselves. The present paper describes a specialized shear testing system, which we have designed and assembled for the purpose of measuring the response of thin single crystal slabs of HgI_2 to shear loading. This mode of loading is especially suitable for studying plastic deformation in single crystal HgI_2 because of its anisotropic, layered structure (as is reviewed briefly later in this section). We have used the system (and are continuing to use it) to determine the shearing response of numerous HgI_2 single crystal test specimens.

Interest in single crystal HgI_2 has been considerable since 1972 when its use as a room-temperature, semiconductor, X-ray detector was reported [6]. For example, in 1983, a single issue of the journal 'Nuclear Instruments and Methods' [7] was devoted largely to the characterization of single crystal HgI_2 and its potential uses in X-ray and gamma ray detection systems; a recent international symposium [8] was also primarily devoted to HgI_2. Its attractiveness is owing to the fact that it is capable of operating as a radiation detector at room temperature. There are thus numerous potential applications for replacing systems which presently require cryogenic cooling (e.g. medical applications involving the use of radio isotopes, military and space applications, scientific uses, etc.) [7–9]. A major problem in the production of HgI_2 radiation detectors is how to increase the yield of good detectors (i.e. reduce the yield of poor detectors) fabricated from a given parent crystal. With a view towards this end, numerous studies have been made to characterize chemical impurities [10–12], stoichiometry [13–17], and crystalline imperfections [1–3, 5, 18–22].

With regard to the present work, the mechanical properties of HgI_2 (and their eventual correlation with detector efficacy) are of practical interest for several reasons. Crystal imperfections, such as dislocations, are considered detrimental to the performance of HgI_2

*This work is based upon parts of the PhD Dissertation of Gary Georgeson, University of California, Santa Barbara, USA.

0022–2461/88 $03.00 + .12

as a detector [22]; studies of crystal plasticity can reveal the nature of the dislocation structure in the crystals; dislocations are found in the as grown material and changes in the dislocation structure are quite possibly induced (inadvertently) by deformation during detector fabrication; an understanding of the influence of stresses upon the dislocation structure can aid in developing optimum processing methods. Also, in passing, we mention that single crystals of HgI_2 have been grown in microgravity in space on a NASA Space Lab mission and are again scheduled to be grown on a future Space Lab mission. Since the space grown crystals are unavoidably subjected to stress upon re-entry into the earth's atmosphere, it is important to understand the influence of stress in order to be able to evaluate the space grown crystals properly. Furthermore, comparisons between the plastic response of the space and terrestrial grown crystals can help to evaluate potential differences between the crystals; such comparisons are planned for future study.

In the present paper, we analyse our data in terms of a two-parameter semiempirical model for plastic yielding that we have developed as an analytic, comparative, and descriptive tool. The model was described briefly in [5], where it was used to analyse uniaxial loading data. Here we show that it generates theoretical stress–strain curves that are in excellent agreement with our shear test data; we also provide a more complete description of the model, including an interpretation of the model parameters, based upon the dislocation structure in HgI_2 proposed by James and Milstein [2].

In their axial compression tests, James and Milstein [2] observed three characteristic responses, i.e. (case a) when the direction of load is parallel to the (0 0 1) slip planes, the material responds elastically until failure occurs by buckling and delamination; (case b) when the direction of load is perpendicular to the (0 0 1) slip planes, the material responds elastically until the crystal shatters by brittle fracture, with no macroscopically observed plastic deformation; (case c) for all other loading directions (not included in cases a or b), the crystals were easily plastically deformed by slip of the (0 0 1) planes; this slip process was also characterized by work-hardening. (It is interesting to note that, while the crystals behave like brittle glass in one mode of loading, they seem more like butter in most other modes of loading.) Atomically, the (0 0 1) slip planes can be considered as triatomic layers of IHgI; i.e. the crystal structure is a layered sequence of monoatomic planes, perpendicular to the [0 0 1] axis, in the order . . . IHgIIHgIIHgI . . . ; bonding between two successive I-layers (thought to be mainly van der Waals) is weak and thus plastic deformation by slip of (0 0 1) planes is easy. James and Milstein [2] explained their experimental results in terms of the following dislocation structure. "(i) There exist easily moved dislocations or dislocation segments, the cores of which are parallel to the (0 0 1) crystallographic planes; these are termed 'easy glide' dislocations. (ii) Although the easy glide dislocations can move readily on (0 0 1) planes, individual easy glide dislocations do not climb out of their (0 0 1) slip planes. (iii) There exist relatively immobile dislocations or dislocation segments ('hard glide' dislocations) that intersect the (0 0 1) planes. The cores of the hard glide dislocations are parallel to the {1 0 0} planes. These dislocations are relatively immobile in the sense that a large resolved shear stress is required in order to move them. (iv) The two types of dislocations (i.e. 'easy' and 'hard' glide) are the only dislocations that contribute to plastic deformation; however, under almost all modes of loading, plastic deformation occurs by slip of the easy glide dislocations. (v) When the easy glide dislocations move on the (0 0 1) planes, they interact with the hard glide dislocations. The interaction interferes with the movement of (or 'pins') the easy glide dislocations, thus causing work hardening."

In our semiempirical model for plastic yielding, the distribution function for the relative density of mobile easy glide dislocations as a function of shear stress is taken to be a normalized Gaussian. The experimentally determined Gaussian parameters are shown to reflect prior work hardening and time-dependent recovery of work hardening in HgI_2 crystals.

2. Shear testing system

Figs 1 to 4 illustrate the essential features of the shear testing system that was designed and assembled for the purpose of measuring the shearing response of single crystal HgI_2 specimens that are in the form of thin slabs. The samples are glued between upper and lower plates, as illustrated in Figs 1 and 2. The lower plate is mounted on the sample platform (see Figs 2 and 3), which is itself part of a Unitron model GME-5 microgoniometer (see Fig. 3) that has been modified to serve as a fixture in the shear testing system. The sample platform is driven forward (i.e. "to the left" in Figs 1 and 3 and "upward" in Fig. 2) by rotation of a micrometer screw. The forward motion of the upper plate is resisted by a pin that is part of a load cell assembly. The force exerted on the pin (i.e. the shear force exerted on the crystal sample) is measured by the load cell system (containing a 5 lb (1 lb = 0.454 kg) Lebow model 3108-5 load cell and model 7525 transducer) and recorded on the Y axis of an X–Y recorder (see Fig. 4); the load cell is securely mounted in the microgoniometer, as illustrated in Fig. 3. The load cell is compensated for off axis loading (i.e. is resistant to extraneous bending and side loading forces) and has a resolution of better than 0.05% of full scale. The shear stress s applied to the specimen is the shear force divided by the (0 0 1) surface area of the crystal sample (i.e. the area of the surface of the sample viewed in Fig. 2). The displacements of the upper and lower

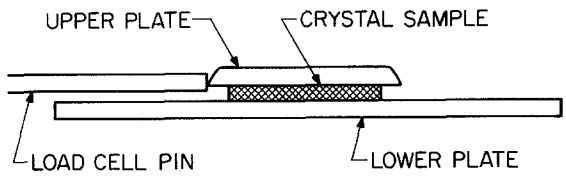

Figure 1 Side view of crystal mounted between upper and lower plates with load cell pin in contact with upper plate. The [0 0 1] crystallographic axis of the sample is normal to the surfaces of the upper and lower plates (and to the axis of the load cell pin).

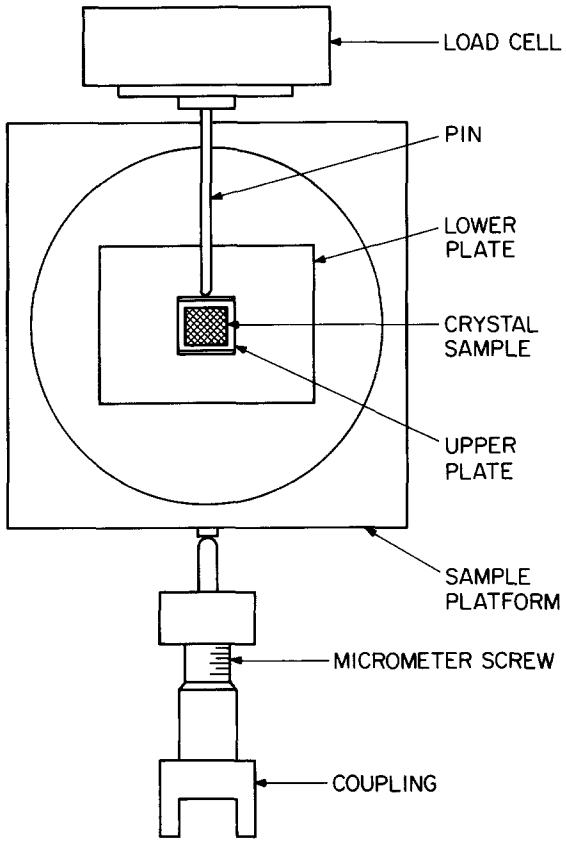

Figure 2 Top view of sample platform containing crystal sample mounted between upper and lower plates.

plates (see Fig. 1) are monitored by electronic gauge heads (Mitutoyo model 599-988); one gauge head is in contact with the upper plate and the other with the lower plate (see Fig. 4); the displacement of the upper plate is electronically subtracted from that of the lower plate in an amplifier (Brown and Sharpe model 1020) and recorded on the X axis of the X–Y recorder (see Fig. 4); the system can determine the difference between measurements, over five English and five metric ranges, of 0.0005 in to 0.000005 in (1 in = 2.54 cm) and 0.01 mm to 0.0001 mm, respectively; the relative displacement (of the bottom plate with respect to the top plate) is divided by the thickness of the crystal sample (i.e. the vertical dimension of the sample viewed in Fig. 1) to obtain the shear strain ε. Shear strains of 0.0001 could be measured for a sample of 1 mm thickness.

During the measurement of a stress–strain curve, the sample platform is driven forward at a constant rate. The strain rate is controlled by rotating the micrometer screw via a servo motor and tachometer in series with two 50:1 gear reductors that provide a net 2500:1 reduction of the angular velocity of the micrometer screw (with respect to that of the motor). In this manner, a range of feed rates of 0.01 to 10 μm sec^{-1} can be achieved; generally tests were run at a feed rate of 1 μm sec^{-1} (which corresponds to a strain rate of about 10^{-3} sec^{-1} for a sample of 1 mm thickness). The shear testing fixture also has a rotary stage (see Fig. 3) and a second micrometer screw (not shown in Figs 2 or 3), oriented perpendicular to the micrometer screw shown in Fig. 2 (this second micrometer screw controls movement of the sample platform to the left and to the right in Fig. 2); this feature is useful for aligning the specimen prior to testing. The shear testing fixture has the capability of rotating the crystal sample (by some prescribed angle θ about the c axis of the sample). Thus, e.g., a shear stress can be applied initially along a [1 0 0] axis, say, and then (by a simple rotation) along some other axis (making an angle θ with respect to the [1 0 0] axis). This is a convenient feature for use in the study of the Bauschinger effect and related phenomena.

The glue used to mount the sample between the upper and lower plates is Sauereisen No. 31 (Sauereisen Cements Co., Pittsburgh, PA); this glue was selected as optimum after experiments were carried out with numerous other glues. The major advantages of this glue are (i) it is strong, (ii) it adheres well to many substances (including HgI_2), and (iii) it has a high modulus of elasticity and is brittle (i.e. its deformation is negligible compared with that of the crystal sample). The only apparent disadvantage is that the surface of the HgI_2 tends to react slightly with the glue after several weeks; this problem is overcome by not allowing the time between application of the glue and testing to exceed 3 days. The upper and lower plates are made of clear plexiglass (in order to be able to visually observe the quality of the adhesive layers between the

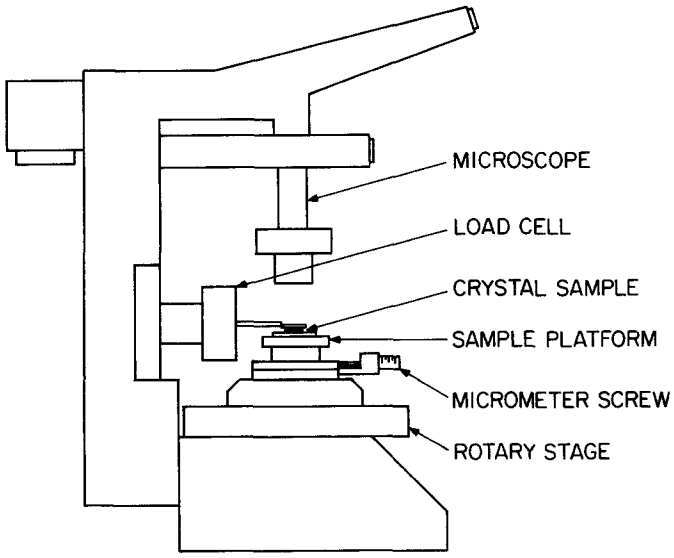

Figure 3 Side view of shear testing fixture.

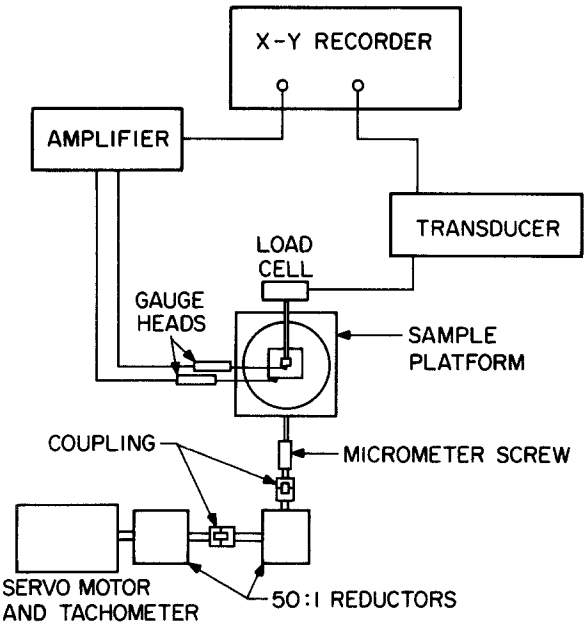

Figure 4 Schematic diagram of shear testing system.

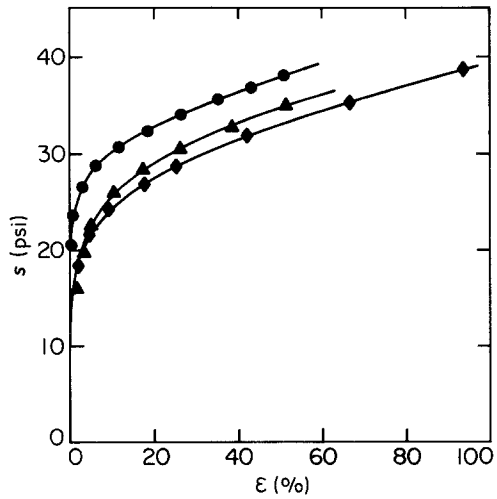

Figure 5 Representative experimental stress–strain data, for thin, single crystals slabs of HgI_2 (◆ sample 1, ▲ sample 2, ● sample 3), taken with the shear testing system described in Section 2 and illustrated in Figs 1–4 and corresponding theoretical curves are based upon the Gaussian model described in Section 3.2.

specimen and the plates). Prior to applying the glue, a razor was used to cut cross-hatched grooves in the lower surface of the upper plate and the upper surface of the lower plate, after roughening these surfaces with # 60 sandpaper. This was done to ensure a good joint between the glue and the plexiglass. The typical size of HgI_2 samples used in our studies is about 9 mm × 9 mm × 0.7 mm; samples with thicknesses as low as 0.3 mm and as high as 1.0 mm and areas as low as 35 mm^2 and as high as 208 mm^2 were also tested. It is desirable to keep the thickness small in order to avoid placing a substantial torque on the sample during loading. No systematic variation of behaviour with sample thickness was observed in the range of thicknesses employed. The method of sample preparation is similar to that of James and Milstein [2].

3. Results and discussion

3.1. Experimental stress–strain relations

Examples of stress–strain data generated in the manner described in the prior section are shown in Fig. 5. (Although the experimental data are recorded continuously on the X–Y recorder, selected experimental points are shown in this figure to distinguish the experimental data from the theoretical stress–strain curves computed using the semiempirical model described in the next subsection.) Experimentally, shear strains of many hundreds of percent are readily obtained with the test system. The typical shearing response of HgI_2 consists essentially of (a) an initial range of shear stress that causes negligibly small plastic deformation (this range is about 10 to 20 psi (1 psi = 6.895 MPa) for the samples of Fig. 5), (b) a middle range in which the onset of appreciable plastic deformation is observed and in which the shear strain increases rapidly and non-linearly with increasing shear stress (and therefore the density of the *mobile*, easy glide dislocations that are responsible for plastic deformation presumably continues to increase as the shear stress increases), and (c) a "final" range in which the shear stress varies linearly with shear strain (it is presumed that, in this region, the density of *mobile*, easy glide dislocations has reached a steady state value). The term "mobile", as used here, refers specifically to dislocations that are *currently* moving, as distinct from those that may have been moving but have become stationary (e.g. by pinning) or those that are capable of moving at increased stress levels, but have not yet become mobile. In the next subsection, we describe a theoretical model that incorporates these experimentally observed features (and their interpretations).

3.2. Theoretical model

The central feature of the theoretical model that we use to analyse the shearing response of single crystal HgI_2 is that a normalized Gaussian distribution

$$f(s) = \frac{1}{\sigma(2\pi)^{1/2}} \exp\left[-(s - s_0)^2/2\sigma^2\right] \qquad (1)$$

characterizes the plastic deformation process. In particular, if n represents either the density of (i) slip planes that are actively slipping when the stress–strain curve has reached its steady state region or of (ii) mobile, easy glide dislocations at steady state, then the quantity $n \int_0^{s_1} f(s)\,ds$ represents, respectively, either the density (i) of slip planes that are actively slipping at any stress s_1 or (ii) of easy glide dislocations that are mobile at stress s_1. In other words, $f(s)\,ds$ can be interpreted to mean either (i) the fraction of newly active slip planes (relative to the number of active slip planes at steady state) that are generated when the stress is increased from s to $s + ds$ or (ii) the relative density of easy glide dislocations (relative to the steady state density) that become newly mobile when the stress is increased from s to $s + ds$. Both interpretations (i) and (ii) are mechanistic and both lead to the same phenomenological conclusions, although (ii) is consonant with microscopic theory of plastic deformation and work hardening in HgI_2 [2]; thus, in our discussions, we shall use the terminology of interpretation (ii). The increment of plastic shear strain $d\varepsilon_p$ that

the crystal undergoes when the stress is increased from s to $s + ds$ is given by

$$d\varepsilon_p = \left(\frac{d\varepsilon_p}{ds}\right)_{ss} \left(\int_0^s f(\xi)\, d\xi + f(s)\right) ds \quad (2)$$

The total plastic deformation ε_p at stress s is computed by integration of Equation 2, i.e.

$$\varepsilon_p(s) = \left(\frac{d\varepsilon_p}{ds}\right)_{ss} \int_0^s d\zeta \left(\int_0^\zeta f(\xi)\, d\xi + f(\zeta)\right) \quad (3)$$

In practice the integrations are carried out numerically. The quantity $(d\varepsilon_p/ds)_{ss}$ is a constant equal to the rate of change of plastic shear strain with shear stress in the steady state region of the stress–strain curve. (If s is a stress in the steady state region, $f(s)$ is essentially zero and $\int_0^s f(\xi)\, d\xi$ is essentially unity; then Equation 2 reduces to

$$\frac{d\varepsilon_p}{ds} = \left(\frac{d\varepsilon_p}{ds}\right)_{ss}$$

in agreement with experiment.) The quantity

$$\left(\frac{d\varepsilon_p}{ds}\right)_{ss} \left(\int_0^s f(\xi)\, d\xi\right) ds$$

represents the contribution to $d\varepsilon_p$ from dislocations that had already become mobile by the time the stress s is reached and

$$\left(\frac{d\varepsilon_p}{ds}\right)_{ss} f(s)\, ds$$

is the contribution to $d\varepsilon_p$ from dislocations that become newly mobile when the stress is increased from s to $s + ds$. Numerical analysis of the stress–strain curves consists of determining the values of the Gaussian parameters σ and s_0 and the steady state work hardening rates (expressed as $(d\varepsilon_p/ds)_{ss}^{-1}$) that yield a best least squares fit between the theoretical and experimental stress–strain curves.

3.3. Comparison between experiment and theory

The empirical parameters determined in the manner described above for the theoretical stress–strain curves shown in Fig. 5 are listed in Table I and the corresponding Gaussian distributions are shown in Fig. 6. The agreement between theory and experiment is seen to be excellent. This description permits the characterization of yielding in the crystals in terms of two convenient parameters, σ and s_0, where σ is the standard deviation of the distribution $f(s)$ and, at the stress $s = s_0$, the density of mobile dislocations has reached half its steady state value. The agreement between

TABLE I Model parameters for the stress–strain curves shown in Fig. 5

Crystal sample	s_0 (psi)	σ (psi)	$\left(\frac{d\varepsilon_p}{ds}\right)_{ss}^{-1}$ (psi)	$s_c = s_0 - 2\sigma$ (psi)
1	28.5	6.6	112	15.3
2	31.7	7.7	99	16.3
3	31.1	4.4	142	22.3

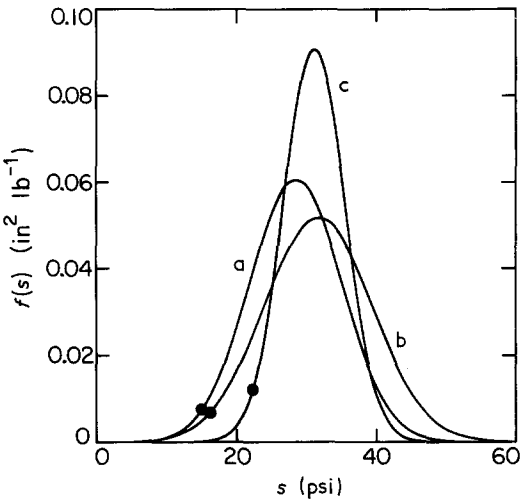

Figure 6 Normalized Gaussian distribution functions used to compute the respective theoretical stress–strain relations shown in Fig. 5. The distribution functions are determined by the parameters s_0 and σ listed in Table I; the respective values of s_c are indicated by the symbols "●". (a sample 1, b sample 2, c sample 3)

theory and experiment seen in Fig. 5 is typical for data taken from the shear loading of samples made from a multitude of HgI_2 single crystals and tested with various orientations of applied c plane stress. For example, samples 2 and 3 of Fig. 5 were prepared from the same parent crystal, which was different from that of sample 1; the directions of shear loading in samples 1, 2, and 3, respectively, were at angles of 3°, 18°, and 35° with respect to the [1 0 0] axis. (The results of experimental studies, of the influence of orientation, within the c plane, upon the shearing behaviour of single crystal HgI_2, will be presented separately.) Another useful parameter, derivable from s_0 and σ is $s_c \equiv s_0 - 2\sigma$; when the shear stress $s = s_c$, according to this model, the density of mobile dislocations has reached about 2% of its steady state value; thus, the value of s_c is a good measure of the onset of yielding. The points $s = s_c$ are marked (in Fig. 6) on the distribution functions used to describe the stress–strain curves in Fig. 5. For the three samples of Fig. 5, sample 1 evidently yielded at a slightly lower stress than sample 2, and both yielded at a considerably lower stress than sample 3 (s_c of sample 1 = 15.3 psi < s_c of sample 2 = 16.3 psi < s_c of sample 3 = 22.3 psi). The value of σ is a measure of the "width" of the transition from elastic deformation to steady state plastic deformation; as this transition narrows, σ decreases; if this transition were to narrow to the point where the stress–strain curve were to consist only of a linear elastic region and a linear plastic region (with a "sharp" yield point at the intersection of the two regions), the "width" σ of the Gaussian would approach zero (the distribution function would, in effect, become a Dirac δ-function at the yield stress). For the three samples of Figs 5 and 6, the region of transition from negligible mobile dislocations to a steady state density of mobile dislocations occurred over a slightly narrower stress range in sample 1 than in sample 2 and over a considerably narrower stress range in sample 3 (σ of sample 2 = 7.7 > σ of sample

TABLE II Influence of work hardening upon model parameters of single crystals of HgI_2 subjected to successive shear loadings. The "initial model parameters" were determined from stress–strain data taken during the initial loading, which work hardened the specimens to the indicated "work hardening stress". After the initial loading, the load was reduced to zero and then reapplied; the "work hardened model parameters" were determined during this second loading

Sample	Initial model parameters (psi)			Work hardened model parameters (psi)			Work hardening stress (psi)
	σ	s_c	s_0	σ	s_c	s_0	
A	5.3	13.6	24.2	3.3	23.8	30.4	30.3
B	6.0	14.5	26.5	3.4	31.0	37.8	36.8
C	5.2	14.0	24.4	3.2	28.0	34.4	33.0
D	4.4	22.3	31.1	2.7	33.6	39.0	38.7
E	3.5	11.8	18.8	2.1	20.2	24.4	24.6
F	2.7	12.9	18.3	2.1	23.6	27.8	27.0

1 = 6.6 > σ of sample 3 = 4.4). The two parameter Gaussian model is seen to provide a useful means of *quantitatively* describing the onset of plastic deformation and the non-linear region of transition from the elastic to the linear, steady state, plastic stress–strain response in the HgI_2 single crystals subjected to shear loading. It is well suited to our particular purposes of comparing and characterizing the yielding behaviour of single crystals that (i) have been grown under a variety of circumstances and (ii) exhibit a gradual transition from elastic to plastic deformation, without evidence of a sharp yield point or critical resolved shear stress. It is also useful for studying the influence of processing variables, such as the effects of work hardening or recovery, as is discussed below.

3.4. Influence of work hardening and recovery on model parameters

Work hardening by plastic deformation is known [2, 3] to increase the yield stress and sharpen the "yield point" in single crystal HgI_2. This phenomenon is examined quantitatively in terms of our model in Table II. Each of the six samples listed in this table was stressed in shear loading to the indicated "work hardening stress," during which time the stress–strain data were taken for determining the initial model parameters. A second set of model parameters was subsequently determined for each work hardened specimen, from data taken while shearing the specimen a second time, in the same direction. Samples A and B were prepared from the same crystal, but were loaded in different directions within the c plane; samples C and D were from the same crystal and were loaded in the same direction (sample D in Table II is the same as sample 3 in Table I); samples E and F were from different crystals and were loaded in different orientations. As expected, in all cases, work hardening causes σ to decrease (the "yield point" becomes sharper) and s_0 and s_c to increase (the "yield stress" becomes greater). Also, in each case, the work hardened value of s_0 is very close to the work hardening stress. This suggests that s_0 can be interpreted as a "bulk yield strength", whereas s_c is a good representation of the "onset of yielding", as mentioned earlier. For the work hardened samples of Table II, s_c is about 80–90% of the work hardening stress. This suggests that prior plastic deformation in a specimen can be recognized by a relatively high value of s_0 combined with a low value of σ; the relationship will be explored quantitatively in subsequent studies.

For the data reported in Table II, the single crystal HgI_2 samples were loaded, unloaded, and soon after unloading, were reloaded. The process of recovery, after loading, can also be studied quantitatively using the shear testing system for data collection and the Gaussian model for data analysis. Detailed quantitative studies of work hardening and recovery will be carried out in due course; illustrative examples are given in Tables III and IV and in Figs 7 and 8. Table III shows how the model parameters change as the sample is work hardened, with three minute intervals between successive shear loadings. The three normalized Gaussians corresponding to the data of Table III are shown in Fig. 7. With each successive loading, both s_c and s_0 increase and σ decreases, as expected. However, with longer time intervals between loadings, substantial recovery of work hardening occurs, as is seen in Table IV and Fig. 8. In particular, the sample of Table IV and Fig. 8 behaved "as expected" upon loading the second time (3 min after the first loading) and upon loading the fourth time (1 min after the third loading); i.e., in each of these loadings, the specimen (which had been work hardened in the preceding loading) exhibited larger values of s_0 and s_c and a smaller value of σ than in the preceding loading. However,

TABLE III Model parameters of a single crystal subjected to three successive shear loadings, with a three minute time interval between loadings. The steady state work hardening rate $(d\varepsilon_p/ds)_{ss}^{-1}$ = 99 psi for all loadings. The "work hardening stress" is the shear stress applied to the sample in the preceding loading

Loading	Work hardening stress (psi)	s_0 (psi)	σ (psi)	s_c (psi)
1st	–	31.7	7.7	16.3
2nd	34.7	38.5	7.1	24.3
3rd	40.2	44.6	5.8	33.0

TABLE IV Model parameters of a single crystal subjected to four successive shear loadings, with different time intervals between each loading. The steady state work hardening rate $(d\varepsilon_p/ds)_{ss}^{-1}$ = 113 psi for all loadings

Loading	Work hardening stress (psi)	s_0 (psi)	σ (psi)	s_c (psi)	Time between loadings
1st	–	18.3	2.7	12.9	
2nd	27.0	27.8	2.1	23.6	3 min
3rd	32.4	30.9	3.9	23.1	20 h
4th	36.1	37.6	3.1	31.4	1 min

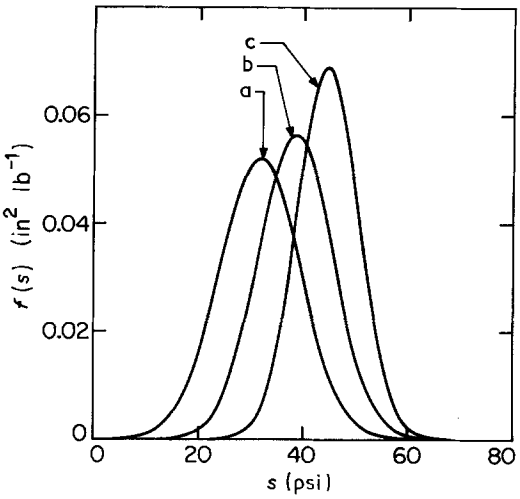

Figure 7 Influence of work hardening upon the normalized Gaussian distribution functions of single crystal HgI_2 subjected to shear loading; the model parameters are listed in Table III. The crystal sample was initially sheared while data for determining the first distribution function were taken; after a three minute interval (from the time of removal of the load), the crystal (which was work hardened by the initial loading) was sheared a second time and a second distribution function was determined; the process was repeated in a third loading. (a first loading, b second loading, c third loading)

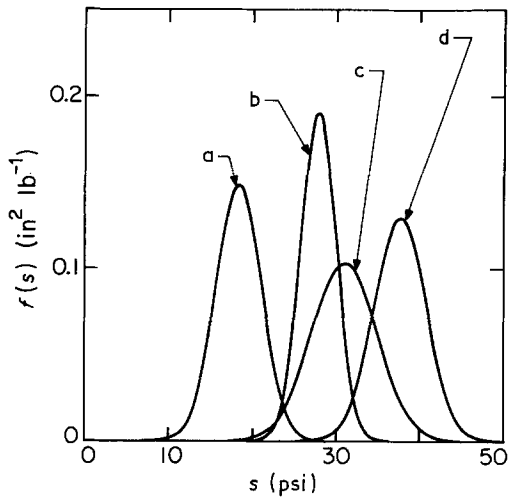

Figure 8 Influence of work hardening and recovery upon the normalized Gaussian distribution functions of single crystal HgI_2 subjected to shear loading; the model parameters are listed in Table IV. The times allowed to elapse between successive loadings were 3 min between the first and second, 20 h between the second and third, and 1 min between the third and fourth. (a first loading, b second loading, c third loading, d fourth loading)

between the second and third loading (during the 20 h time interval), the normalized Gaussian distribution function of the sample evidently underwent a large increase in width (i.e. σ of the third loading is greater than σ of the second loading), although the mean stress s_0 is about what would be expected (i.e., in the third loading, $s_0 = 30.9$ psi, which is close to the work hardening stress of 32.4 psi that was applied 20 h before the third loading). It is of particular interest to note that the values of s_c are almost the same in the second and third loadings. This behaviour can be understood in terms of the dislocation model of James and Milstein [2], in which work hardening occurs when the easy glide dislocations, moving on (0 0 1) planes, are pinned by the hard glide dislocations. Recovery is represented by an "unpinning" resulting from thermal excitation; the larger the localized internal stress in the neighbourhood of "tangles" or "pile-ups" of pinned dislocations, the easier it will be for thermal excitation to unpin the dislocations. Only a fraction of the dislocations can be expected to become unpinned (the fraction will depend upon prestress, temperature, and time). Those dislocations that do become unpinned will, upon successive loading, begin to move (in response to the load) at lower stresses than those that have not become unpinned. Thus, as thermal excitation causes unpinning of easy glide dislocations, the value of s_c of a work hardened sample naturally decreases. This is what occurred during the 20 h recovery period between the second and third loadings of the sample of Table IV and Fig. 8. Since most of the dislocations that became pinned during work hardening are likely not to become unpinned by thermal excitation, the value of s_0 is not likely to change significantly during recovery (since s_0 is a measure of "bulk yielding"). Because the Gaussian is normalized (i.e. $\int_0^\infty f(s)\,ds = 1$), increasing s_c while keeping s_0 approximately fixed results in a lowering of its amplitude $f(s_0)$.

In summary, we have designed, built, and tested an experimental apparatus for the purpose of measuring the response of thin HgI_2 single crystals to shear stresses. Initial tests have been made of shear stress against shear strain on thin, single crystal slabs of HgI_2 vapour grown at EG&G, Santa Barbara Operations. The results are analysed in terms of a two parameter semiempirical model for yielding that fits the experimental data extremely well. The model assumes that the distribution function $f(s)$ for the fraction of dislocations (on the (0 0 1) planes) that become newly mobile when the stress is increased from s to $s + ds$ is given by a normalized Gaussian with a mean stress s_0 and standard deviation σ. When the stress $s = s_0$, half of the ultimately active dislocations on the (0 0 1) planes will have commenced movement. The "onset of yielding" is identified as $s_c \equiv s_0 - 2\sigma$; at stress $s = s_c$, approximately 2% of the ultimately active dislocations are mobile. The parameters σ and s_0 are determined numerically from a best least squares fit to the experimental data. The utility of the model for studying work hardening and time dependent recovery has been established. Work hardening causes s_c and s_0 to increase and σ to decrease; during recovery, s_c and σ increase while s_0 evidently changes very little. This behaviour is understood in terms of the dislocation model for pinning "(0 0 1) dislocations" by "{1 0 0} dislocations" [2]. The shear testing system and theoretical model will be used for extensive studies of the shear response of single crystal HgI_2, including tests of radiation detectors of various grades of quality, the orientation dependence of the stress–strain response in the (0 0 1) plane, work hardening, time dependent relaxation, and successive loadings in different directions.

Acknowledgement

The crystals tested in the present study were grown from the vapour phase at EG&G, Inc., Santa Barbara Operations, by the method described in [23]. We are grateful to the State of California MICRO program and EG&G, Inc., for support of this work (NASA, H-78559B; DOE, DE-AC08-83 NV10282). Particular thanks are due to Mr W. Schnepple, Dr L. van den Berg, Ms C. Ortale, and Dr M. Schieber for helpful discussions and invaluable assistance.

References

1. T. W. JAMES and F. MILSTEIN, *J. Mater. Sci.* **16** (1981) 1167.
2. *Idem, ibid.* **18** (1983) 3249.
3. F. MILSTEIN, B. FARBER, K. KIM, L. VAN DEN BERG and W. F. SCHNEPPLE, *Nucl. Instrum. Meth.* **213** (1983) 65.
4. G. GEORGESON and F. MILSTEIN, *Rev. Sci. Instrum.* **54** (1983) 1026.
5. F. MILSTEIN and G. GEORGESON, in "Dislocations in Solids Some Recent Advances AMD" Vol. 63, edited by X. Markenscoff (ASME, 1985) p. 89.
6. H. S. MALM, *IEEE Trans. Nucl. Sci.* **NS-19** (1972) 263.
7. *Nucl. Instrum. Meth.* **213** (1983).
8. Sixth International Workshop-Compound Semiconductors for Room Temperature X-ray and Nuclear Detectors, Davos, Switzerland, Sept. 14–19, 1987. (Proceedings to be published).
9. M. SCHIEBER, M. ROTH and W. F. SCHNEPPLE, *J. Cryst. Growth* **65** (1983) 353.
10. T. KOBAYASHI, J. T. MUHEIM, P. WAEGLE and E. KALDIS, *J. Electrochem. Soc.* **130** (1983) 1183.
11. J. T. MUHEIM, T. KOBAYASHI and E. KALDIS, *Nucl. Instrum. Meth.* **213** (1983) 39.
12. I. F. NICOLAU, *J. Biochem. Technol.* **33A** (1983) 350.
13. *Idem, J. Cryst. Growth* **48** (1980) 45.
14. G. DISHON, M. SCHIEBER, L. BENDOR and L. HALITZ, *Mater. Res. Bull.* **16** (1981) 565.
15. M. C. DELONG and F. ROSENBERGER, *ibid.* **16** (1981) 1445.
16. A. TADJINE, D. GOSSELIN, J. M. KOEBEL and P. SIFFERT, *Nucl. Instrum. Meth.* **213** (1983) 77.
17. A. BURGER, M. ROTH and M. SCHIEBER, *J. Cryst. Growth* **56** (1982) 526.
18. W. B. YELON, R. W. ALKIRE, M. SCHIEBER, L. VAN DEN BERG, S. E. RASMUSSEN, H. CHRISTENSEN and J. R. SCHNEIDER, *J. Appl. Phys.* **52** (1981) 4604.
19. A. LEVI, A. BURGER, M. SCHIEBER, L. VAN DEN BERG, W. B. YELON and R. W. ALKIRE, *Nucl. Instrum. Meth.* **213** (1983) 31.
20. S. GITS and A. AUTHIER, *J. Cryst. Growth* **58** (1982) 473.
21. S. GITS, *Nucl. Instrum. Meth.* **213** (1983) 43.
22. M. SCHIEBER, C. ORTALE, L. VAN DEN BERG, W. SCHNEPPLE, L. KELLER, C. N. J. WAGNER, W. YELON, F. ROSS, G. GEORGESON and F. MILSTIEN (to be published in the proceedings of [8]).
23. M. SCHIEBER, W. F. SCHNEPPLE and L. VAN DEN BERG, *J. Cryst. Growth* **33** (1976) 125.

Received 14 September 1987
and accepted 26 January 1988